The Effect of Cr, Co, Al, Mo, and Ta on a Series of Cast Ni-Base Superalloys on the Stability of an Aluminide Coating During Cyclic Oxidation in Mach 0.3 Burner Rig

Isidor Zaplatynsky and Charles A. Barrett
Lewis Research Center
Cleveland, Ohio

October 1986

NASA

THE EFFECT OF Cr, Co, Al, Mo, AND Ta ON A SERIES OF CAST Ni-BASE SUPERALLOYS ON THE STABILITY OF AN ALUMINIDE COATING DURING CYCLIC OXIDATION IN MACH 0.3 BURNER RIG

Isidor Zaplatynsky and Charles A. Barrett
National Aeronautics and Space Administration
Lewis Research Center
Cleveland, Ohio 44135

SUMMARY

The influence of varying the content of Co, Cr, Mo, Ta, and Al in a series of cast Ni-base γ/γ' superalloys on the behavior of aluminide coatings was studied in burner rig cyclic oxidation tests at 1100 °C. The alloys had nominally fixed levels of Ti, W, Cb, Zr, C, and B. The alloy compositions were based on a full 2^5-fractional statistical design supplemented by 10 star point alloys and a center point alloy. This full central composite design of 43 alloys plus two additional alloys with extreme Al levels allowed a complete second degree estimating equation to be derived from the 5-compositional variables. The weight change/time data for the coated samples fitted well to the paralinear oxidation model and enabled a modified oxidation attack parameter, K_a' to be derived to rank the alloys and $\log K_a'$ to be used as the dependent variable in the estimating equation to determine the oxidation resistance of the coating as a function of the underlying alloy content. The most protective aluminide coatings are associated with the highest possible base alloy contents of Cr and Al and at a 4 percent Ta level. The Mo and Co effects interact but at fixed levels of 0, 5 or 10 percent Co a 4 percent Mo level is optimum.

INTRODUCTION

The effect of compositional changes in Ni-base γ/γ' superalloys on the behavior of aluminide coatings has been subject of several investigations (refs. 1 to 9). Also a concise but complete review of this work was published recently by Tomaszewicz and Wallwork (ref. 10). There is agreement that the substrate composition has a major effect on the coating behavior. Many studies (refs. 2 to 4, 7 and 8) suggest that beneath the external β-NiAl layer an inner layer is formed by outward diffusion of nickel and alloying elements from the substrate layer. This inner diffusion zone consists of columnar grains of either β-NiAl or γ-Ni$_3$Al interdispersed by regions rich in the tungsten, molybdenum, chromium and columbium existing as intermetallic compounds and carbides of these refractory metals. However, the formation of carbides in the base alloy was found by Fleetwood (ref. 4) to be undesirable because they often penetrated the coating, offering an easy path for oxidation.

The exact mechanism of coating degradation remains a point of contention. Early work seemed to suggest that diffusion of aluminum into a substrate alloy was responsible for the degradation. This point of view is supported by the more recent work of Smialek and Lowell (ref. 8). The other point of view is (ref. 5) that in the case of aluminide coatings on nickel-base superalloys, the continuous spalling and reforming of the oxide scale are the main reason for their degradation. It has been established by several investigators that coating degradation is a function of substrate composition (refs. 1,3,4,6,9). It

has been suggested (ref. 6) that the refractory metal phases might act as a diffusion barrier reducing aluminum diffusion into the substrate and the outward diffusion of nickel or alloying elements into the coating, and thus decreasing coating degradation. Except for the work of Talboom and Petrusha (ref. 1) on the single and binary additions to pure nickel on the diffusional stability of NiAl coatings, the work in this area is rather limited.

The study described herein is a part of the Conservation of Strategic Aerospace Materials (COSAM) program. Its objective has been to investigate the effect of Cr, Co, Al, Mo, and Ta contents in a typical Ni-base superalloy on the stability at an aluminide coating during cyclic oxidation in a Mach 0.3 burner rig. The alloys had nominally fixed levels of Ti, W, Cb, Zr, C, and B. The alloy compositions were based on a full 2^5-fractional statistical design supplemented by 10 star point alloys and a center point alloy. This full central composite design of 43 alloys plus two additional alloys with extreme Al levels was used by Barrett (ref. 11) to derive a complete second degree equation that described the effect of compositional changes on the cyclic oxidation behavior of these alloys.

The aluminide coating was applied by the RT-21[a] process. Cyclic oxidation tests were performed in a Mach 0.3 burner rig for 150 and 300 1-hour cycles with a sample temperature of 1100 °C. Weight change of the specimens was determined by removing them periodically from the burner rig and weighing. After testing, the specimens were subjected to metallographic and x-ray diffraction analyses.

MATERIALS AND EXPERIMENTAL PROCEDURES

Preparation of the Specimens

The basic levels of the five compositional variables are schematically designated as 0,1,2,3, and 4 where the 2 values are the center point of the design. Table I shows the actual weight percent (wt %) corresponding to the five levels. The basic composition of the prototype alloy was: Ni-balance, Ti-1.0 wt %, W-2.0 wt %, Cb-1.0 wt %, Zr-0.10 wt %, B-0.01 wt %, C-0.12 wt %. The five levels chosen for the five alloying elements represent their range in commercial alloys. Thus, the center point alloy designated as (22222) would be the basic composition with the five varied levels Al-4.75 wt %, Cr-12.0 wt %, Co-10.0 wt %, Mo-2.0 wt %, and Ta-4 wt %. Similarly the alloy coded (00113) has the basic composition with Al-3.25 wt %, Cr-6.0 wt %, Co-5.0 wt %, Mo-1.0 wt %, and Ta-6.0 wt %.

The master heats of the alloys were prepared by vacuum induction melting by Howmet Turbine Components Corporation of Dover, New Jersey as 3 in. diameter ingots, each weighing approximately 40 lb.

The master heat ingots were then used to make individual investment frame castings (vacuum induction melted) by Duradyne Technologies, Inc. of Mentor, Ohio. Included on each frame were 12 round coating bars: 12 tensile/stress

---

[a]Trade name of Chromalloy American Corporation.

rupture bars, 12 round burner rig bars, and 16 rectangular oxidation leaves. The burner rig bars were 3/8 in. diameter and 4 in. long. Table II lists the actual compositions of each alloy. In all cases the actual compositions were within 10 percent of the target compositions. The aluminide coating was applied to all specimens by the RT-21 process.

BURNER RIG TESTING

The Mach 0.3 burner rig used in these tests has been described in reference 12. Eight specimens were placed in a carousel holder which was rotated at 400 rpm in front of the burner nozzle. The centers of the specimens were evenly spaced on a 4.2 cm (approx. 1-3/8 in.) diameter circle. In this cyclic oxidation test, the specimens were heated for 1 hr and then cooled with a stream of compressed air for 3 min. The burner rig was fired at a fuel-to-air ratio of about 0.05 using Jet A fuel and combustion air preheated to 260 °C (500 °F). Test temperature was 1100±20 °C (2012 °F) as determined with a calibrated (for emissivity and window absorption) disappearing filament optical pyrometer when focusing on the center of the hot zone of the specimens facing the nozzle of the burner.

The back side (facing away from the nozzle) of the specimens was hotter than the front face by 20 °C. Only the central part of the specimens was exposed to the flame. All alloys were tested for 150 1-hr cycles. Fifteen of the alloys were also tested for 300 1-hr cycles. The weight of each specimen was monitored periodically by removing it from the holder and weighing. Orientation of each specimen with regard to the nozzle was maintained. Thermogravimetric data were recorded as total weight change (Δw) versus the number of cycles. Weight change per unit area (Δw/A) was not used because the longitudinal distribution of temperature on the specimens was not uniform. The most heavily oxidized region was the central part of the specimens with an area of about 4 cm.^{2} Two specimens of each alloy were tested at the same time and the average value of Δw was used in the analysis. After testing, XRD patterns were taken from the cylindrical surface of the specimens (one specimen per alloy) in order to identify the phases present on the oxidized surface. The same specimens were plasma sprayed with copper for edge preservation and cross sectioned through the center of the hot zone for metallographic examination to ascertain the oxidation damage and accompanying microstructural changes.

RESULTS AND ANALYSIS

Metallography

Metallographic examination of the specimens in the as-coated condition revealed that the coating consisted of two layers (fig. 1). The outer layer, about 40 μm thick, is a large grained NiAl (β) with Cr, Mo, and Co in solid solution. The inner layer contained MC, $M_{23}C_6$ or M_6C carbides and sigma phase in a columnar matrix of NiAl + Ni_3Al (ref. 3). The substrate was composed of Ni solid solution (γ) with very fine precipitates of Ni_3Al (γ'). During cyclic oxidation all the alloys showed an initial weight gain (tables III and IV) but after about 40 cycles some alloys began to lose weight faster than others. Figure 2(a) illustrates typical changes that took place during cyclic oxidation testing of the alloys. Here, in the case of Alloy 16, after 150 cycles, the

3

columnar zone has disappeared and its original location is marked by the presence of carbide and sigma phase grains. NiAl formed large grains separated from the substrate by a layer of Ni_3Al. The Ni_3Al precipitates in the substrate became coarser and the 40 μm thick zone of the substrate near the original substrate-coating interface was depleted of Ni_3Al. The same alloy (fig. 2(b)) when subjected to 300 1-hr oxidation cycles underwent similar but more extensive changes. The amount of NiAl was significantly reduced and Ni_3Al precipitates in the substrate grew in size. XRD analyses of the oxide scales (in situ) revealed the presence of Al_2O_3, NiAl(β), $Ni_3Al(\gamma')$, Ni ss(γ) and on several occasions a aluminate spinel structure was detected. The Ni ss was formed on the surface of the coatings as result of aluminum loss from Ni_3Al, which, in turn was also the product of aluminum loss from NiAl. No simple relationships can be drawn regarding the stability of the aluminide coating as a function of alloy composition based on the examination of thermogravimetric data, metallographic and XRD analyses and therefore it is necessary to make use of a statistical approach.

REGRESSION ANALYSIS

The oxidized coated bars were separated into two groups for purposes of analysis. In the first group the samples were tested for 150 hr and in the second for 300 hr. The weight change time data for the 150 hr run for each alloy is listed in table IV. These values are the average of two samples for each alloy.

Initially, for the 150 hr data set the entire test interval of weight change/time data was fitted for each alloy to a paralinear model equation (11)

$$\Delta w = k_1^{1/2} t^{1/2} - k_2 t \pm \sigma \tag{1}$$

Where k_1 is the parabolic scaling constant, k_2 is a linear spalling constant and σ is the standard deviation of the Δw estimate. The rejection level was set at 0.90 (i.e., if either coefficient is not significant at this level it is dropped and the regression equation is recomputed).

Note here that this is not a specific weight change equation since the weight was not divided by a surface area. This lead to a modified attack parameter defined as

$$K_a' = (k_1^{1/2} + 10. \, k_2) \tag{2}$$

These equations have been discussed previously in references 12 and 14 to 16. The derived coefficients, $k_1^{1/2}$ and k_2, the coefficient of determination, R^2 and σ values for equation (1) are listed in table V for each alloy. The K_a' estimates from equation (2) are also listed.

The data fitted for each alloy represents the average of two samples (designated a and b) run together as replicates on the eight-sample carousel. In general the weight changes tended to follow in tandem i.e. the individual sample curves had similar shapes, with time with one sample either lagging or leading. These average curves tended to be classically paralinear in nature

4

(i.e., they start out parabolic in nature, reach a gradual maximum and drop at nearly a linear rate). This was true for all the alloys tested except for alloy G-42. Note that its k_2 coefficient was such as to make the weight change curve more positive. When in the K_a' calculation the absolute value of k_2 is used it makes no difference in this calculation even though the weight change curve is quite different (i.e., not paralinear).

In most cases the fit was excellent with R^2 values well over 90 percent. In six cases the fit was fair to good with values between 80 to 90 percent. However, two alloys, G-41 and G-31, had fits that were relatively poor with R^2 values of 38.8 and 49.5 percent respectively. Figures 3 and 4 show the individual sample weight change values for G-41 and G-31 along with the paralinear curve fit vector line along with the $\pm 1-\sigma$ error lines for the average of the two samples as given in table III. Compared with these are figures 5 and 6 for individual samples G-6 and G-24 which represent fits in the mid 80 percent R^2 value range and those with fits of >90 percent, respectively. Figure 7 shows the samples G-42A and G-42B along with the derived average vector line. Here as discussed above the k_2 component makes the curve more positive.

The poor fit in figure 3 is due primarily to the divergence of the individual sample curves. In this case it is difficult to decide which sample is truly representative of the alloy. Figure 4 on the other hand shows the samples behaving similarly but with a high degree of scatter. Figures 5 and 6 are more typical of the general body of data with the samples moving together and the scatter decreasing.

The K_a' values range from a minimum value of 0.1763 for alloy G-41 to a maximum value of 10.706 for alloy G-1. This represents virtually no attack at the lowest K_a' value to catastrophic oxidation for the G-1 alloy. For reasons above, however, the low K_a' value for G-41 is questionable due to the individual sample divergence.

Where possible, thickness change measurements were made on the test samples at the completion of the 150 hr test. These values are also listed in table V. They represent the total diameter change in microns. In earlier studies the attack parameter has correlated well with thickness change measurements. This nearly linear relationship is shown in figure 8. Because in many ways a K_a' type parameter is a better measurement of corrosion attack than thickness change (refs. 13 and 14), the thickness change measurement is used more as a confirmation of the K_a' type analytical approach.

Derived K_a' values were fitted as a function of alloy chemistry according to the following second degree multiple linear regression estimating equation using the log K_a' transformation (ref. 15) where the elemental symbols stand for weight percent of each alloy constituent:

$$\log K_a' = Ao + b_1Al + b_2Cr + b_3Co + b_4Mo + b_5Ta$$

$$+ b_6Al^2 + b_7Cr^2 + b_8Co^2 + b_9Mo^2 + b_{10}Ta^2$$

$$+ b_{11}Al \cdot Cr + b_{12}Al \cdot Co + b_{13}Al \cdot Mo + b_{14}Al \cdot Ta \qquad (3)$$

$$+ b_{15}Cr \cdot Co + b_{16}Cr \cdot Mo + b_{17}Cr \cdot Ta$$

$$+ b_{18}Co \cdot Mo + b_{19}Co \cdot Ta + b_{20}Mo \cdot Ta \pm \sigma$$

A version of equation (3) was also used which included linear terms for the slight degree of variability for supposedly fixed elements Ti, Nb, W, Zr, and C but these terms were, as expected, not significant.

Equation (3), was analyzed by means of the statistical software package MINITAB, release 81.1 on an IBM 370 main frame computer. In addition all the compositional variables were first "centered" by subtracting the mean of the weight percent of each compositional variable from each individual compositional value for each sample. This tends to minimize the correlation between linear and higher order terms sometimes leading to bias in estimating the coefficients (17).

The forward selection method was used with a rejection F- value of 2.88 or a probability 90 percent. This gave the following regression equation

$$\log K_a' = 0.27160 - 2.0005W - 0.04169Cr - 0.021120Co - 0.00698Ta^2 \pm 0.2709 \quad (4)$$

with an R^2 of 38.8 percent. However, alloy G-41 gave a very high standardized residual of -4.25 σ units indicating a probable outlier. Because of the problems with this sample discussed above its K_a' was discarded and the entire regression equation recomputed. This gave the following estimating equation:

$$\log K_a' = 0.17654 - 0.026523Co - 0.04314Cr + 0.03873Ta^2 - 0.08464Al$$
$$- 0.07264Mo - 0.04884Al^2 + 0.01062Mo \cdot Co \pm 0.1647 \qquad (5)$$

The R^2 increased to 74.0 percent. For this data set of 43, only three values were flagged as possible outliers but they are close to being within an acceptable $\pm 2\sigma$. Figure 9 shows a plot of the predicted versus observed K_a' values in terms of log values. Figure 10 shows the standardized residuals versus the log K_a' estimated values. The randomized nature of the data are another indication of the validity of equation (5). Figure 11 plots the converted antilogs of values estimated by equation (5) versus the observed K_a' values listed in table VI. The diagonal line shows the perfect fit line along with the computed average deviation values.

Based on the derived K_a' estimates for the standard 43 alloy design the minimum predicted value is for alloy G-37. However, special alloy G-45 with an Al level higher than the designed alloys has the lowest overall predicted oxidation attack.

It is possible to use the derived regression equation and predict the lowest attack rate over the range of alloy compositions. This was done for

6

three typical Cr levels which should be as high as possible for maximum pro-
tection as indicated by the regression coefficients. The results are shown in
table VII for three typical Co levels of 0, 5, and 10 percent and for Cr levels
of 8, 12, and 16 percent. A detailed analysis of equation (5) at these 9 com-
binations of Cr and Co levels shows the Al level should be as high as possible-
here 6.25 percent. The Ta level is optimum due to the Ta^2 term at its mean
value near 4 wt %. The ideal Mo values are partly dependent on the Co com-
position. At Co levels of 0, 5, and 10 wt % Co, a Mo level of 4 wt % gives
the minimum K_a' values.

An additional series of runs were made on selected samples for a total of
300 hr. This data is listed in table IV with the values again listed for the
average of two samples tested during the same run. In general this longer time
data would be expected to fall within the error bars of the vector extended
from 150 to 300 hr unless breakaway had occurred (16). Breakaway is a sharp
downward break in the ΔW/time curve associated with a less protective oxide
becoming rate controlling. If breakaway takes place, the weight change values
should drop well below the error bars of the predicted curve. Of the twenty-
eight-300 hr runs, ten fell below the 1 σ band at 300 hr, 15 were above, and
3 were within. Of the 10 that fell below the error band, the question is
whether the low estimates are due to scatter, breakaway or a combination of
both. If it is breakaway then the original K_a' value is probably too low.
X-ray diffraction results of the two sets of samples show no difference with
time, NiO might have shown up in the spall, however. Figure 11 is typical of
breakaway in a paralinear oxidation process when spalling becomes excessive.

In summary the above results suggest that for this series of Ni-base γ/γ'
superalloys that the best cyclic oxidation burner rig resistance conferred by
an aluminide coating is associated with the highest levels of Cr and Al. Ta is
optimum at 4 wt %. The Mo content is related to the Co level. At typical Co
compositions of 0 to 10 percent Co a 4 wt % Mo level is optimal. It was sug-
gested (ref. 6) that certain elements including Ta, Cr, and Mo tend to inhibit
the diffusion of Ni into the NiAl or more likely the back diffusion of Al from
the NiAl into the alloy. This enables the NiAl coating to confer a high degree
of cyclic oxidation resistance with the low scaling rates associated with
Al_2O_3 formation along with low oxide spalling rates.

CONCLUDING REMARKS

B-NiAl coatings on a series of Ni-base γ/γ' superalloys with 45 system-
atic variations in the substrate alloy of Cr, Co, Al, Mo, and Ta were tested
in cyclic oxidation at 1100 °C in a Mach 0.3 burner rig. In tests of 150 to
300 hr the best of the alloys exhibited the same type of paralinear oxidation
behavior as plain B-NiAl with both low scaling and spalling rates associated
with Al_2O_3 formation. An oxidation attack parameter derived from the sample
weight change/time data was used to determine the effect of the 5 alloy ele-
ments by regression analysis. The results indicate the Cr and Al should be as
high as possible. The Ta level is optimum at a midrange of 4 percent. The Co
and Mo interact but if typical Co levels of 0 to 10 percent are fixed the high-
est Mo level tested of 4 percent is the most beneficial.

7

REFERENCES

1. Talboom, F.P.; and Petrusha, J.A.: Superalloy Coatings for Components of Gas Turbine Engine Applications. AFML-TR-66-15, Feb. 1966.

2. Goward, G.W.; Boone, D.H.; and Giggins, C.S.: Formation and Degradation Mechanisms of Aluminide Coatings on Nickel-Base Superalloys. Transactions of ASM, vol. 60, no. 2, 1967, pp. 228-241.

3. Redden, T.K.: Ni-Al Coating-Base Metal Interactions in Several Nickel-Base Alloys. Trans. of Met. Soc. of AIME, vol. 242, no. 8, Aug. 1968, pp. 1695-1702.

4. Fleetwood, M.J.: Influence of Nickel-Base Alloy Composition on the Behaviour of Protective Aluminide Coatings. J. Inst. Met. vol. 98, no. 1, 1970, pp. 1-7.

5. Goward, G.W.: Current Research on the Surface Protection of Superalloys for Gas Turbine Engines. J. Met., vol. 22, no. 10, 1970, pp. 31-39.

6. Nejedlik, J.F.: Development of Improved Coatings for Nickeland Cobalt-Base Alloys. AFML-TR-70-208, Aug. 1970.

7. Goward, G.W.; and Boone, D.H.: Mechanisms of Formation of Diffusion Aluminide Coatings on Nickel-Base Superalloys. Oxid. Met., vol. 3, no. 5, 1971, pp. 475-495.

8. Smialek, J.L.; and Lowell, C.E.: Effects of Diffusion on Aluminum Depletion and Degradation of Ni-Al Coatings. J. Electrochem. Soc., vol. 121, no. 6, June 1974, pp. 800-805.

9. Zaplatynsky, I.: The Effect of Cobalt Content in U-700 Type Alloys on Degradation of Aluminide Coatings. NASA TM-87173, 1985.

10. Tomaszewicz, P.; Wallwork, G.R.: The Degradation of Alumina-Forming Coating Systems on Nickel, Cobalt and Iron-Based Alloys by High Temperature Oxidation. Rev High Temp. Mater., vol. 5, no. 1, 1982, pp. 49-91.

11. Hancock, E.W.: Transitions from Parabolic to Linear Kinetics in Scaling of Metals. J. Electrochem. Soc., vol. 106, no. 9, Sept. 1959, pp. 771-775.

12. Barrett, C.A.: The Effects of Cr, Co, Al, Mo, and Ta on the Cyclic Oxidation Behavior of a Prototype Cast Ni-Base Superalloy Based on a 2^5 Composite Statistically Designed Experiment. High Temperature Corrosion in Energy Systems, M.F. Rothman, ed., Metallurgical Society of AIME, 1985, pp. 667-680.

13. Gray, H.R.; and Sanders, W.A.: Effect of Thermal Cycling in a Mach 0.3 Burner Rig on Properties and Structure of Directionally Solidified $\gamma/\gamma'-\sigma$ Eutectic. Conference on In Situ Composites, M.R. Jackson, et. al., eds., Xerox Individualized Publishing. 1976, pp. 201-210.

14. Barrett, C.A.; and Lowell, C.E.: Resistance of Nickel-Chromium-Aluminum Alloys to Cyclic Oxidation at 1100 ° and 1200 °C. NASA TN D-8255, 1976.

15. Barrett, C.A.; Miner, R.V.; and Hull, D.R.: The Effects of Cr, Al, Ti, Mo, W, Ta, and Cb on the Cyclic Oxidation Behavior of Cast Ni-Base Superalloys at 1100 ° and 1150 °C. Oxid. Met., vol. 20, no. 5/6, 1983, pp. 255-278.

16. Lowell, C.E.; Smialek, J.L.; and Barrett, C.A.: Cyclic Oxidation of Super-alloys. High Temperature Corrosion, NACE-6, R.A. Rapp, ed., National Association of Corrosion Engineers, 1983, pp. 219-226.

17. Ryan, T.: Centering Data. MINITAB User's Group Newsletter, no. 4, June 1984, pp. 1-2.

TABLE I. - ALLOY CODE LEVELS CONVERTED
TO TARGET COMPOSITIONS FOR
PROTOTYPE ALLOY

[Ni-balance, Ti-1.0 wt %,
W-2.0 wt %, Cb-1.0 wt %,
Zr-0.10 wt %, B-0.01 wt %,
C-0.12 wt %. (G-1 to G-43)].

Alloy code/wt %					
	0	1	2	3	4
Al	3.25	4	4.75	5.50	6.25
Cr	6	9	12	15	18
Co	0	5	10	15	20
Mo	0	1	2	3	4
Ta	0	2	4	6	8

TABLE II. - INGOT CHEMISTRY FOR PROTOTYPE Ni-BASE
TEST ALLOYS WITH VARYING Al, Cr, Co, Mo
and Ta LEVELS[a]

G	Al	Cr	Co	Mo	Ta	Ni
1	3.86	8.99	4.94	0.98	1.99	75.03
2	3.95	8.95	14.83	1.01	1.99	65.05
3	4.20	15.41	4.82	.97	2.14	68.47
4	3.87	13.73	14.67	.98	2.11	60.53
5	5.30	9.07	4.99	.99	2.01	73.43
6	5.43	9.05	15.12	1.01	1.98	63.14
7	5.47	15.10	5.09	1.02	2.02	67.03
8	5.43	15.14	15.25	1.02	2.01	56.86
9	3.92	9.05	4.98	.94	5.94	71.01
10	4.06	8.97	15.21	1.07	6.00	60.58
11	4.01	15.06	4.93	1.10	5.98	64.84
12	4.03	14.70	14.66	1.05	5.82	55.65
13	5.46	9.09	4.98	.97	6.01	69.29
14	5.74	8.27	15.84	.97	6.30	58.76
15	5.70	15.07	4.57	1.06	6.15	63.34
16	5.49	15.20	15.10	.99	6.02	52.91
17	3.97	9.00	5.04	2.97	2.02	72.79
18	3.98	8.93	14.95	2.97	1.92	63.05
19	3.98	14.96	5.02	3.03	2.03	66.73
20	4.05	14.91	14.88	3.08	1.96	56.92
21	5.44	9.08	5.10	3.00	2.02	71.17
22	5.45	9.00	14.95	3.02	2.00	61.36
23	5.47	15.05	5.03	3.03	2.05	65.04
24	5.58	15.09	15.08	3.08	1.97	54.89
25	3.98	8.93	4.92	2.86	5.98	69.19
26	4.05	8.70	15.34	2.83	5.74	59.25
27	4.11	14.84	4.93	2.92	5.99	63.01
28	4.11	15.09	14.80	2.96	6.01	52.78
29	5.51	8.90	4.85	2.87	5.90	67.86
30	5.47	9.02	15.01	2.92	6.07	57.31
31	5.50	15.00	5.05	2.98	6.01	61.27
32	5.55	15.02	15.00	2.96	6.06	51.15
33	5.01	12.94	10.68	2.14	4.26	60.53
34	4.77	11.53	10.36	0.0	4.25	65.03
35	4.81	11.98	10.00	3.97	3.83	61.30
[b]36	4.80	6.11	9.99	1.94	4.11	68.89
37	4.85	18.24	10.26	2.00	4.01	56.37

[a]Fixed elements: Ti range 0.92 to 1.09 wt %
W range 1.88 to 2.16 wt %
Cb range 0.90 to 1.06 wt %
Zr range 0.05 to 0.11 wt %
C range 0.08 to 0.12 wt %
B all 0.01 wt %

[b]Lost in remelting for test samples.

TABLE II. - Concluded

G	Al	Cr	Co	Mo	Ta	Ni
38	4.91	11.22	0.0	1.93	4.23	73.71
39	4.88	11.91	20.11	2.01	4.00	52.75
40	4.59	12.70	9.00	1.94	0.0	67.80
41	4.85	11.87	9.91	1.92	7.94	59.35
42	3.54	12.37	10.26	2.20	4.22	62.99
43	6.17	12.13	10.10	2.06	3.74	61.51
44	2.52	11.87	9.89	1.98	4.04	65.51
45	7.09	12.09	10.23	2.09	4.11	60.14

TABLE III. - THERMOGRAVIMETRIC DATA FOR ALUMINIDED COATED NI-BASE γ/γ'

ALLOYS TESTED AT 1100 °C IN A MACH 0.3 BURNER RIG

FOR 150 ONE-HOUR CYCLES

[Average of twin samples tested in same run.]

Alloy G series	ΔW, mgs (Number of cycles)					
1	3.7(10)	2.3(20)	0.0(40)	-5.0(60)	-12.6(100)	-59.0(150)
2	2.3(10)	1.7(20)	-.9(40)	-1.8(60)	-3.6(100)	-9.8(150)
3	1.4(10)	.6(20)	-1.5(40)	-5.0(60)	-9.1(100)	-19.3(150)
4	1.2(10)	1.3(20)	.5(20)	0(60)	-2.4(100)	-13.0(150)
5	1.5(10)	2.1(20)	.2(40)	-2.3(60)	-7.3(100)	-17.2(150)
6	2.0(10)	2.0(20)	.3(40)	-.8(60)	-.8(100)	-3.9(150)
7	2.0(10)	3.2(20)	3.5(40)	4.2(60)	4.7(100)	1.9(150)
8	1.6(10)	2.7(20)	2.9(40)	3.5(60)	4.3(100)	2.8(150)
9	.8(10)	.7(20)	-1.3(40)	-2.3(60)	-8.1(110)	-14.6(150)
10	1.8(10)	1.8(20)	1.2(40)	1.6(60)	-1.7(110)	-4.1(150)
11	4.0(10)	4.9(20)	5.1(40)	5.3(70)	5.0(91)	.5(150)
12	2.5(10)	3.2(20)	3.6(40)	4.9(70)	4.8(91)	4.4(150)
13	3.8(10)	4.7(20)	4.8(40)	4.5(70)	3.5(91)	-1.8(150)
14	2.3(10)	1.9(20)	1.2(40)	.6(70)	-.7(91)	-5.2(150)
15	2.3(10)	2.0(20)	3.0(40)	0 (70)	-4.9(110)	-13.4(150)
16	2.0(10)	2.2(20)	4.1(40)	4.5(70)	4.3(110)	4.0(150)
17	3.2(10)	2.1(20)	3.0(40)	1.4(70)	-1.3(110)	-4.7(150)
18	2.9(10)	2.2(20)	3.4(40)	2.2(70)	-.4(110)	-4.7(150)
19	2.1(10)	3.5(20)	2.8(40)	2.2(60)	2.5(100)	-1.8(150)
20	1.9(10)	3.1(20)	2.5(40)	1.6(60)	3.6(100)	2.5(150)
21	4.4(10)	5.7(20)	4.6(40)	3.4(60)	4.4(100)	1.3(150)
22	5.3(10)	6.5(20)	5.9(40)	5.2(60)	6.9(100)	6.6(150)
23	3.3(10)	2.8(20)	3.2(40)	3.7(60)	4.0(100)	2.5(150)
24	3.2(10)	3.4(20)	3.7(40)	4.4(60)	6.1(100)	6.7(150)
25	4.4(10)	4.6(20)	5.0(40)	4.7(60)	3.3(100)	-2.1(150)
26	3.1(10)	2.7(20)	2.3(40)	1.6(60)	-.7(100)	-6.6(150)
27	2.9(10)	3.0(20)	3.9(40)	3.8(60)	2.0(100)	-1.1(150)
28	2.0(10)	2.1(20)	2.9(40)	2.8(60)	3.5(100)	3.3(150)
29	3.2(10)	3.2(20)	3.4(40)	2.0(60)	-2.8(100)	-6.9(150)
30	2.8(10)	3.3(20)	3.9(40)	4.2(60)	4.3(100)	3.5(150)
31	.8(10)	1.5(20)	1.5(40)	2.1(60)	.3(100)	-.2(150)
32	1.3(10)	1.4(20)	1.5(40)	--------	----------	.9(150)
33	1.2(10)	1.8(20)	3.0(40)	3.7(60)	3.4(100)	-.2(150)
34	.7(10)	.7(20)	-.8(40)	-3.1(60)	-6.5(100)	-15.7(150)
35	.9(10)	1.5(20)	2.1(40)	2.9(60)	2.8(100)	1.3(150)
36	--------	--------	--------	--------	----------	----------
37	.5(10)	1.2(20)	2.2(40)	3.4(60)	3.8(100)	3.0(150)
38	2.2(10)	1.9(20)	.8(40)	-0.6(60)	-2.8(100)	-11.7(150)
39	1.3(10)	1.5(20)	1.9(40)	2.1(60)	2.8(100)	3.1(150)
40	3.1(10)	1.6(20)	-3.4(40)	-7.3(60)	-13.5(100)	-31.8(150)
41	.1(10)	.3(20)	.2(40)	.1(60)	.4(100)	-.7(150)
42	4.1(10)	8.0(20)	15.7(40)	19.9(60)	30.7(100)	38.7(150)
43	2.0(10)	2.3(20)	2.7(40)	1.9(60)	3.4(100)	3.5(150)
44	.6(10)	.1(20)	-.8(40)	-1.6(60)	-3.5(100)	-5.7(150)
45	1.4(10)	2.2(20)	2.4(40)	2.3(60)	3.6(100)	3.4(150)

TABLE IV. – THERMOGRAVIMETRIC DATA FOR ALUMINIDED COATED NI-BASE γ/γ'

ALLOYS TESTED AT 1100 °C IN A MACH 0.3 BURNER RIG

FOR 300 ONE-HOUR CYCLES

[Average of twin samples tested in same run.]

Alloy G series	ΔW, mgs (Number of cycles)					
1	0.2(20)	−2.2(40)	−6.6(100)	−12.0(140)	−21.3(200)	−34.4(300)
3	1.3(20)	0 (40)	−2.3(100)	−7.8(140)	−12.1(200)	−17.2(300)
5	1.1(20)	−.1(40)	−1.9(80)	−7.9(140)	−11.9(200)	−16.0(300)
6	2.6(20)	1.8(40)	1.7(80)	.6(140)	−1.6(200)	−1.6(300)
7	3.4(20)	3.8(40)	2.2(100)	−1.3(140)	−7.8(200)	−14.3(300)
9	2.3(20)	1.8(40)	−.4(100)	−6.8(140)	−15.5(200)	−27.4(300)
10	2.8(20)	2.6(40)	−1.5(100)	−6.6(140)	−11.7(200)	−22.9(300)
12	3.6(30)	4.4(70)	4.4(120)	----------	4.4(200)	−5.0(300)
13	4.1(20)	4.1(40)	1.1(100)	−5.2(160)	−13.7(234)	−18.3(300)
14	4.1(20)	3.6(60)	2.8(100)	1.3(160)	−1.7(234)	−3.1(300)
15	2.5(20)	2.8(40)	.9(100)	−4.3(160)	−16.2(234)	−22.9(300)
16	3.1(20)	3.4(40)	4.9(100)	4.8(160)	3.6(234)	1.2(300)
26	3.3(20)	4.1(60)	3.4(80)	2.4(140)	.3(200)	−4.0(300)
32	2.9(20)	4.2(60)	4.0(80)	4.3(140)	3.3(200)	.9(300)
33	3.9(20)	4.5(40)	4.3(80)	1.4(140)	−.9(203)	−1.3(300)
34	1.4(30)	−1.0(70)	−6.5(120)	----------	−15.5(200)	−32.1(300)
35	4.1(20)	5.3(40)	5.0(80)	3.7(140)	2.4(203)	.6(300)
37	3.7(20)	5.0(40)	4.7(80)	5.0(140)	4.4(203)	4.3(300)
38	1.8(30)	−1.1(70)	−5.2(20)	----------	−13.1(200)	−26.1(300)
39	3.6(20)	4.2(40)	4.0(80)	4.0(140)	3.7(203)	4.0(300)
40	2.7(20)	--------	−18.0(80)	−41.4(140)	−66.3(200)	−82.5(300)
41	3.1(20)	4.1(60)	3.8(80)	3.3(140)	1.0(200)	−3.8(300)
43	4.7(20)	--------	6.5(80)	6.3(140)	4.9(200)	2.6(300)
44	3.3(20)	--------	1.3(80)	−1.9(140)	−6.4(200)	−11.5(300)
45	3.0(20)	4.2(60)	4.1(80)	3.9(140)	3.8(200)	1.2(300)

TABLE V. - CYCLIC OXIDATION CONSTANTS

Alloy G series	Test time, hr	$k_1^{1/2}$	$-k_2$	R^2	σ	K_a'	Δth μ	300 hr^a test data
1	150	4.314	0.6392	85.8	9.05	10.706	320	A
2		.8572	.13050	97.2	.80	2.1622	120	-
3		1.0999	.20948	99.2	.88	3.1947	130	A
4		1.2391	.16644	88.2	1.83	2.9035	150	-
5		1.5052	.23016	99.3	.70	3.8068	200	A
6		.6007	.07141	82.6	.81	1.3148	130	A
7		1.0054	.06080	96.4	.80	1.6134	120	B
8		.7514	.03633	97.6	.60	1.1147	120	-
9		.9688	.17060	99.1	.69	2.6748	130	A
10		.88350	.097911	96.8	.42	1.8626	110	B
11		1.7664	.14003	98.4	.61	3.1667	160	E
12		.88782	.04330	99.1	.42	1.3208	70	B
13		1.81241	.16064	98.5	.51	3.4188	130	B
14		.97379	.11560	97.9	.46	2.1297	180	A
15		1.8304	.22857	96.2	1.14	4.1161	150	A
16		.83149	.03965	99.0	.42	1.2290	---	B
17		1.26733	.13412	97.9	.43	2.6086	190	-
18		1.35936	.13760	96.4	.60	2.7354	190	-
19		1.1764	.10365	94.7	.66	2.2129	180	-
20		.7610	.04709	95.3	.68	1.2319	180	-
21		1.6138	.12461	96.8	.86	2.8599	200	-
22		1.6141	.09449	97.8	1.05	2.5590	120	-
23		.93492	.06051	97.8	.53	1.5400	240	-
24		.79017	.02270	99.0	.54	1.0171	110	-
25		1.84294	.16305	98.4	.55	3.4734	120	-
26		1.36687	.15446	97.9	.53	2.9114	370	A
27		1.2901	.11169	96.1	.64	2.4070	120	-
28		.6665	.03981	85.4	1.15	1.0646	120	-
29		1.4652	.15773	86.9	1.36	3.0425	170	-
30		1.0520	.07148	89.0	1.32	1.7668	180	-
31		.3506	.02584	49.5	1.15	.6090	150	-
32		.49676	.03467	98.2	.25	.8434	---	A
33		.9079	.06759	91.2	.88	1.5838	290	A
34		1.0161	.18162	99.2	.72	2.8323	120	A
35		.55631	.03208	96.4	.47	.8771	100	A
37		.42290	.00993	96.8	.56	.5222	80	E
38		1.3476	.18192	97.1	.96	3.1668	170	A
39		.34978	.00832	99.6	.16	.4330	90	A
40		1.9024	.35516	99.1	1.53	5.4540	250	B
41		.08088	.00955	38.79	.29	.1763	90	B
42		1.3355	-.15924	99.8	1.21	2.9279	170	B
43		.5054	.02063	95.8	.61	.7117	100	E
44		.22728	.05822	98.9	.36	.8094	50	A
45		.47035	.01701	97.8	.44	.6405	80	B
U-700		.3506	.02584	49.5	1.15	.6090	200	B

^{a}Extrapolate 150 hr vector to 300 hr.
  A ΔW is above error band.
  B ΔW is below error band.
  E ΔW is within error band.
  - Not tested.

TABLE VI. – OBSERVED AND DERIVED K_a' VALVES FOR
ALUMINIDE COATED SERIES OF Ni-BASE γ/γ'
SUPERALLOYS TESTED IN A MACH 0.3
BURNER RIG AT 1100 °C FOR 150 HR

Sample	Alloy factor levels					Observed K_a'	Estimated[a] K_a'
	Al	Cr	Co	Mo	Ta		
1	1	1	1	1	1	10.706	5.9001
2	1	1	3	1	1	2.1622	2.5285
3	1	3	1	1	1	3.1947	2.9712
4	1	3	3	1	1	2.9035	1.5310
5	3	1	1	1	1	3.8068	4.6424
6	3	1	3	1	1	1.3148	1.8900
7	3	3	1	1	1	1.6134	2.3608
8	3	3	3	1	1	1.1147	1.0094
9	1	1	1	1	3	2.6748	5.6944
10	1	1	3	1	3	1.8626	2.3902
11	1	3	1	1	3	3.1667	3.0430
12	1	3	3	1	3	1.3208	1.3358
13	3	1	1	1	3	3.4188	4.3956
14	3	1	3	1	3	2.1297	1.8778
15	3	3	1	1	3	4.1161	2.3540
16	3	3	3	1	3	1.2280	.9937
17	1	1	1	3	1	2.6086	3.2521
18	1	1	3	3	1	2.7354	2.3475
19	1	3	1	3	1	2.2129	1.7629
20	1	3	3	3	1	1.2319	1.2714
21	3	1	1	3	1	2.8599	2.4528
22	3	1	3	3	1	2.5590	1.7300
23	3	3	1	3	1	1.5400	1.3169
24	3	3	3	3	1	1.0171	.9047
25	1	1	1	3	3	3.4734	3.3513
26	1	1	3	3	3	2.9114	2.0886
27	1	3	1	3	3	2.4070	1.8292
28	1	3	3	3	3	1.0646	1.2266
29	3	1	1	3	3	3.0425	2.4522
30	3	1	3	3	3	1.7668	1.7388
31	3	3	1	3	3	.6090	1.3403
32	3	3	3	3	3	.8434	.9262
33	2	2	2	2	2	1.5838	1.2412
34	2	2	2	0	2	2.8323	2.1537
35	2	2	2	4	2	.8771	1.0906
36	2	0	2	2	2	Not tested	------
37	2	4	2	2	2	.5222	.7929
38	2	2	0	2	2	3.1668	3.0366
39	2	2	4	2	2	.4330	.8109

TABLE VI. - Concluded

Sample	Alloy Factor Levels					Observed Ka	Estimated[a] Ka
	Al	Cr	Co	Mo	Ta		
40	2	2	2	2	0	5.4540	6.6481
41	2	2	2	2	4	[b].1763	------
42	0	2	2	2	2	2.9279	1.5019
43	4	2	2	2	2	.7117	.9105
44	-1	2	2	2	2	.8094	1.3627
45	5	2	2	2	2	.6405	.5109

[a]Derived from equation (5) with $\log K_a'$ as the dependent variable and converted from $\log K_a'$ estimates.
[b]Outlier-discarded.

TABLE VII. – OPTIMUM LEVELS OF Al, Mo AND
Ta FOR MINIMUM K_a' ESTIMATES AT SELECTED
LEVELS OF Cr AND Co COMPUTED FROM THE

REGRESSION EQUATION

Cr	Co	Al	Mo	Ta	Log K_a'	K_a'-est.
8	0	6.25	4	4	0.03020	1.0720
8	5				.003979	1.0092
8	10				-.02224	.9501
12	0				-.1424	.7204
12	5				-.1686	.6783
12	10				-.1948	.6386
16	0				-.3149	.4843
16	5				-.3411	.4559
16	10	↓	↓	↓	-.3674	.4291

NiAl

NiAl +
CARBIDES +
σ PHASES

NiSS + Ni₃Al

CARBIDES +
σ PHASES

40 μM

(A) ALLOY 41.

NiAL

NiAl +
CARBIDES +
σ PHASES

NiSS + Ni₃Al
(SUBSTRATE)

40 μM
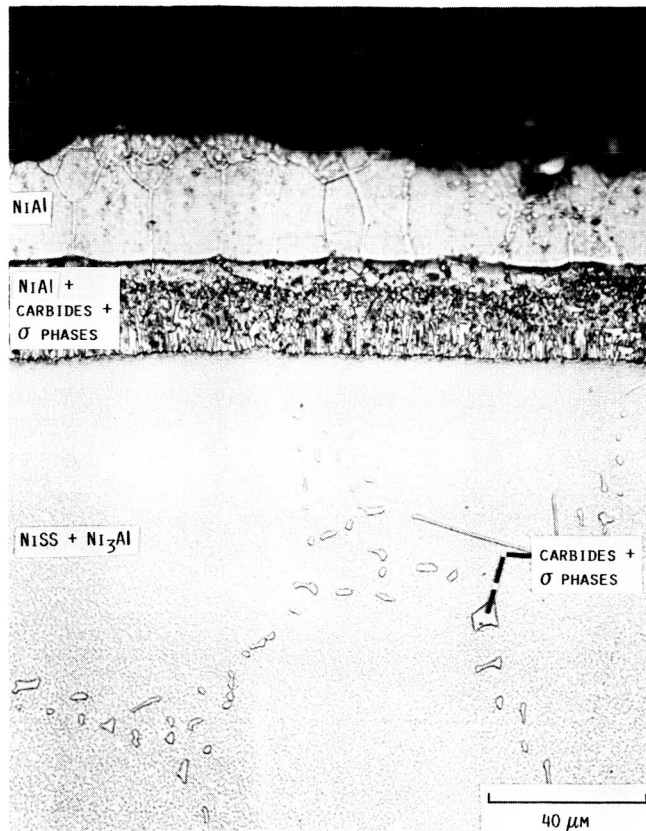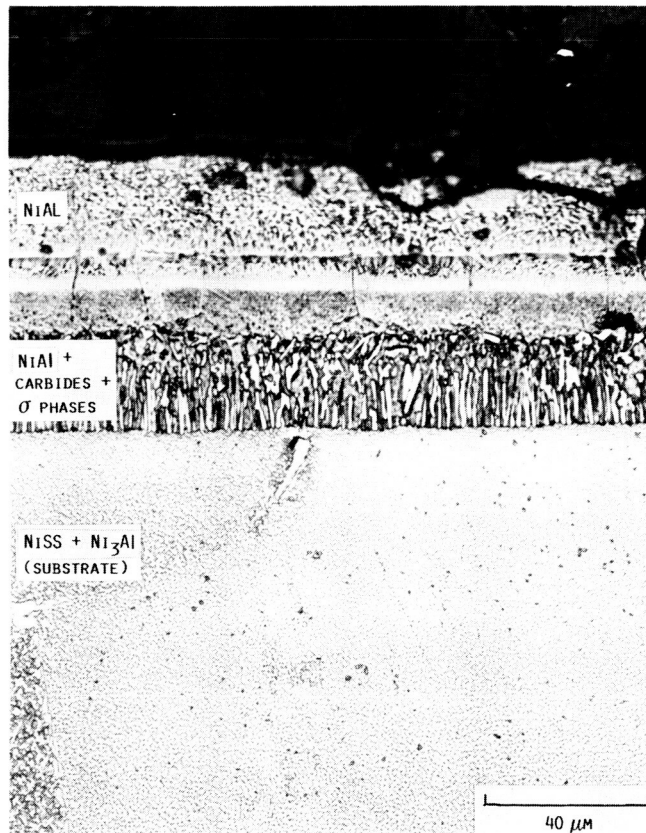
(B) ALLOY 43.

FIGURE 1. - TYPICAL MICROSTRUCTURE OF ALLOYS COATED WITH ALUMINIDE
BY RT-21 PROCESS.
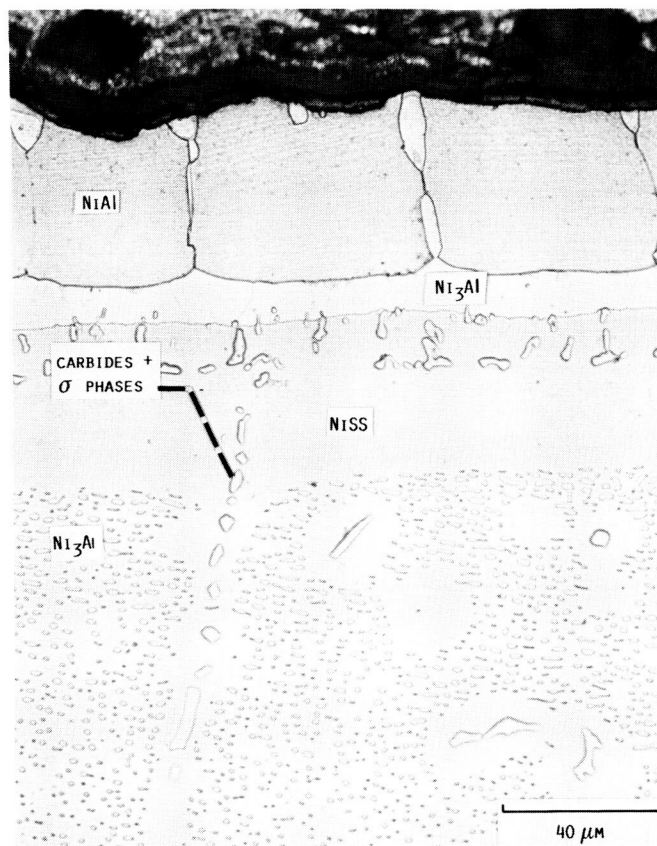
(A) 150 CYCLES.
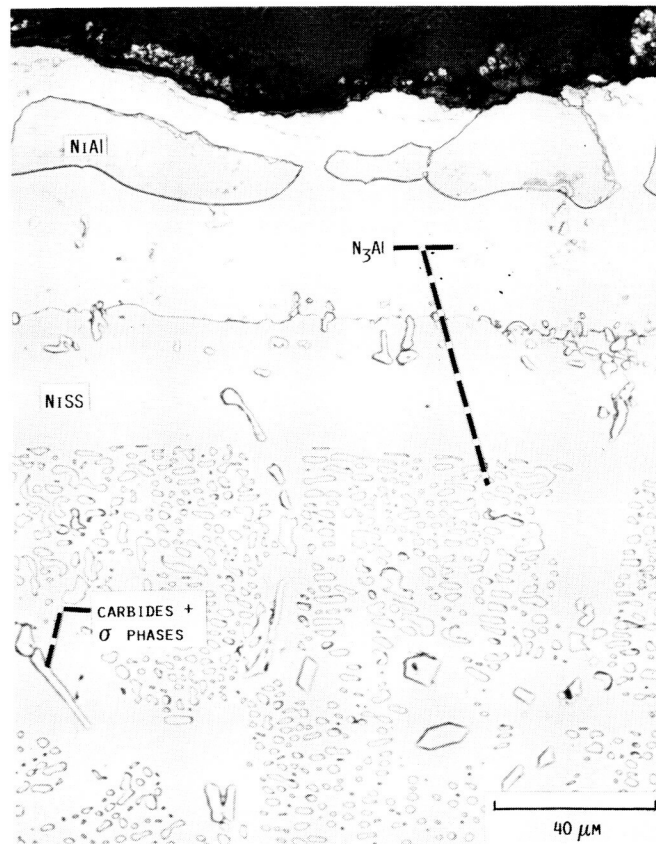
(B) 300 CYCLES.

FIGURE 2. - TYPICAL MICROSTRUCTURE OF ALUMINIDE COATED ALLOY 16 AFTER
150 AND 300 1-HOUR OXIDATION CYCLES AT 1100 °C IN A MACH 0.3 BURNER
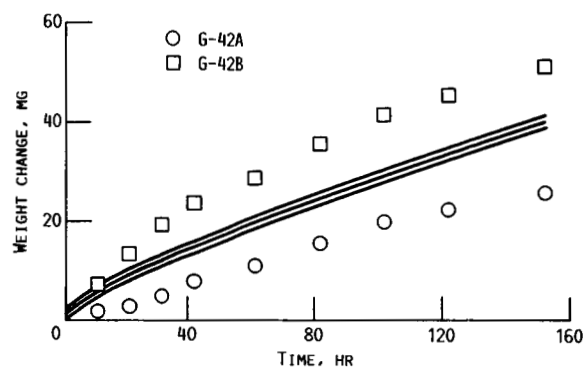RIG.
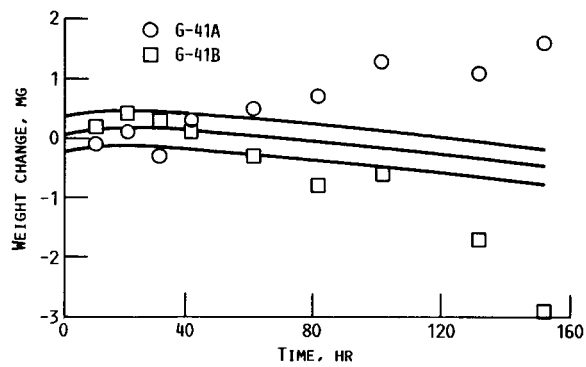
FIGURE 3. – INDIVIDUAL REPLICATE COATED TEST BAR DATA
FOR ALLOY G-41 AND REGRESSION CURVE FIT OF THE AVER-
AGE WEIGHT CHANGE DATA WITH TIME. UPPER AND LOWER
CURVES INDICATE ±1 - σ LIMITS. R^2 = 38.8%.
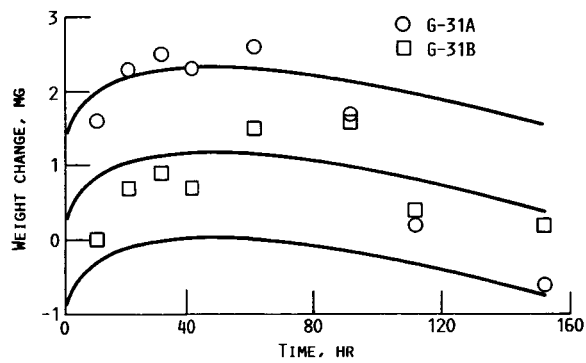
FIGURE 4. – INDIVIDUAL REPLICATE COATED TEST BAR DATA
FOR ALLOY G-31 AND REGRESSION CURVE FIT OF THE AVER-
AGE WEIGHT CHANGE DATA WITH TIME. UPPER AND LOWER
CURVES INDICATE ±1 - σ LIMITS. R^2 = 49.5%.
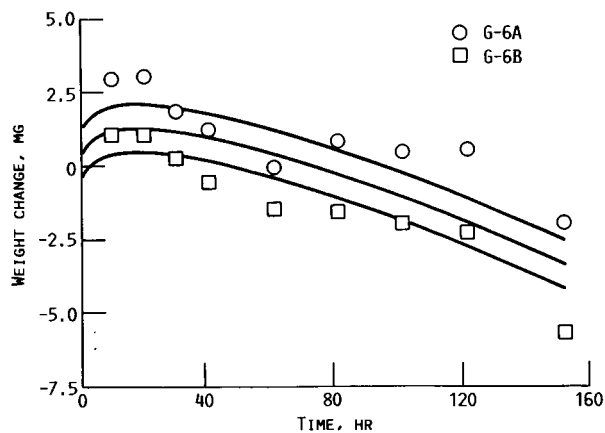
FIGURE 5. - INDIVIDUAL REPLICATE COATED TEST BAR DATA
FOR ALLOY G-6 AND REGRESSION CURVE FIT OF THE AVER-
AGE WEIGHT CHANGE DATA WITH TIME. UPPER AND LOWER
CURVES INDICATE $\pm 1 - \sigma$ LIMITS. R^2 = 82.6%.
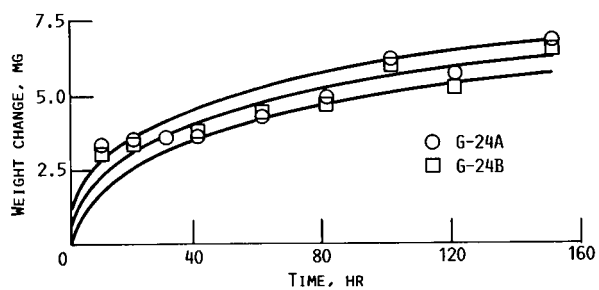
FIGURE 6. - INDIVIDUAL REPLICATE COATED TEST BAR DATA
FOR ALLOY G-24 AND REGRESSION CURVE FIT OF THE AVER-
AGE WEIGHT CHANGE DATA WITH TIME. UPPER AND LOWER
CURVES INDICATE $\pm 1 - \sigma$ LIMITS. R^2 = 99%.

FIGURE 7. - INDIVIDUAL REPLICATE COATED TEST BAR DATA
FOR ALLOY G-42 AND REGRESSION CURVE FIT OF THE AVER-
AGE WEIGHT CHANGE DATA WITH TIME. UPPER AND LOWER
CURVES INDICATE $\pm 1 - \sigma$ LIMITS. R^2 = 99.8%.
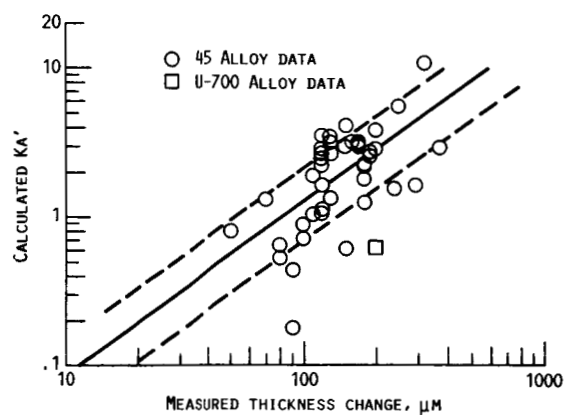
FIGURE 8. - RELATIONSHIP OF K_A' VALUES DERIVED FROM
WEIGHT CHANGE KINETIC DATA FOR 150 HOUR TESTS AND
MEASURED THICKNESS CHANGE. REGRESSION FIT:
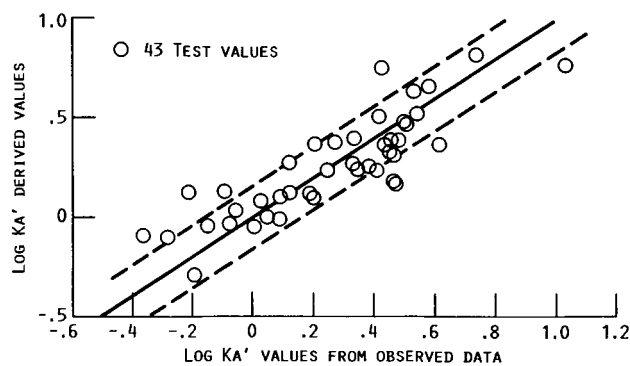LOG K_A' = -2.2650 + 1.1728 LOG $\Delta T \pm 0.2644$.
R^2 = 38.4%.

FIGURE 9. – DERIVED Ka' VALUES FROM REGRESSION FIT OF
EQUATION (3) VERSUS OBSERVED Ka' VALUES. DIAGONAL
SOLID LINE DEFINES PERFECT FIT. UPPER AND LOWER
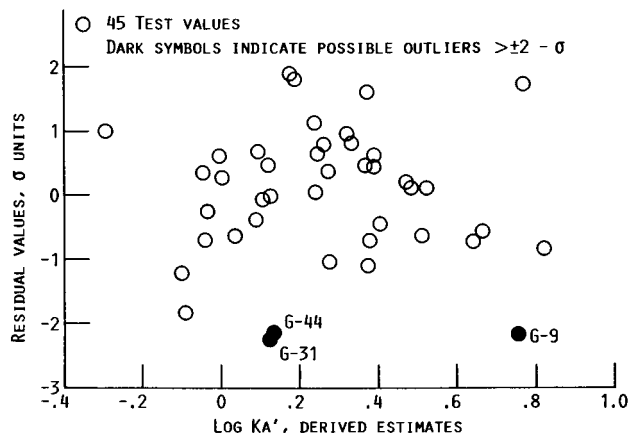DASHED LINES REPRESENT ±1-AVERAGE DEVIATION.

FIGURE 10. – RESIDUALS PLOTTED AGAINST FITTED VALUES OF
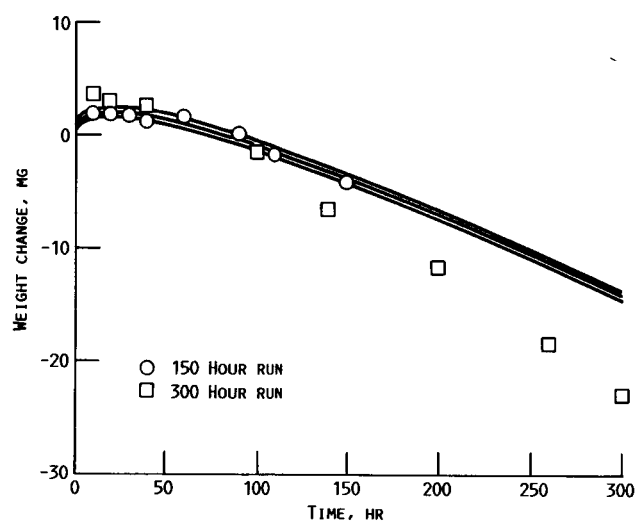Ka' FOR REGRESSION ANALYSIS FOR EQUATION (3).

FIGURE 11. - COMPARISON 150 HOUR TEST DATA FOR ALLOY G-10
AND ITS REGRESSION FIT EXTRAPOLATION TO 300 HOURS WITH
ITS ±1 - σ DEVIATION CURVES COMPARED WITH ACTUAL 300
HOUR DATA FOR THE SAME ALLOY SHOWING APPARENT BREAKAWAY.

1. Report No. NASA TM-88840	2. Government Accession No.	3. Recipient's Catalog No.
4. Title and Subtitle The Effect of Cr, Co, Al, Mo, and Ta on a Series of Cast Ni-Base Superalloys on the Stability of an Aluminide Coating During Cyclic Oxidation in Mach 0.3 Burner Rig		5. Report Date October 1986
		6. Performing Organization Code 505-63-01
7. Author(s) Isidor Zaplatynsky and Charles A. Barrett		8. Performing Organization Report No. E-3007
		10. Work Unit No.
9. Performing Organization Name and Address National Aeronautics and Space Administration Lewis Research Center Cleveland, Ohio 44135		11. Contract or Grant No.
		13. Type of Report and Period Covered Technical Memorandum
12. Sponsoring Agency Name and Address National Aeronautics and Space Administration Washington, D.C. 20546		14. Sponsoring Agency Code

15. Supplementary Notes

16. Abstract

The influence of varying the content of Co, Cr, Mo, Ta, and Al in a series of cast Ni-base γ/γ' superalloys on the behavior of aluminide coatings was studied in burner rig cyclic oxidation tests at 1100 °C. The alloys had nominally fixed levels of Ti, W, Cb, Zr, C, and B. The alloy compositions were based on a full 2^5-fractional statistical design supplemented by 10 star point alloys and a center point alloy. This full central composite design of 43 alloys plus two additional alloys with extreme Al levels allowed a complete second degree estimating equation to be derived from the 5-compositional variables. The weight change/time data for the coated samples fitted well to the paralinear oxidation model and enabled a modified oxidation attack parameter, K_a' to be derived to rank the alloys and $\log K_a'$ to be used as the dependent variable in the estimating equation to determine the oxidation resistance of the coating as a function of the underlying alloy content. The most protective aluminide coatings are associated with the highest possible base alloy contents of Cr and Al and at a 4 percent Ta level. The Mo and Co effects interact but at fixed levels of 0, 5 or 10 percent Co a 4 percent Mo level is optimum.

17. Key Words (Suggested by Author(s)) Superalloys; Nickel aluminide coatings; Cyclic oxidation; Burner rig tests	18. Distribution Statement Unclassified - unlimited STAR Category 26

19. Security Classif. (of this report) Unclassified	20. Security Classif. (of this page) Unclassified	21. No. of pages	22. Price*

*For sale by the National Technical Information Service, Springfield, Virginia 22161